MICROVASCULAR RESEARCH **43,** 46–59 (1992)

Skin Capillary Metrics and Hemodynamics in the Hairless Mouse

HARVEY N. MAYROVITZ

Microvascular and Physiological Studies Unit, Wound Care and Vascular Department, Miami Heart Institute, Miami Beach, Florida 33140

Received April 12, 1990

The transparency of the homozygous hairless mouse ear permits detailed study of the intact skin microcirculation without surgical interventions to the skin tissue. It is useful to study many microvascular phenomena and has the potential to provide data to clarify issues related to human skin microcirculation. The aim of this investigation was to quantify the normal capillary geometric and hemodynamic parameters. In each of 36 capillary pairs (10 mice), capillary diameter (D), length (L), and velocity (V) were measured and blood flow (Q) and shear rate ($S = 8V/D$) were calculated. Loops were chosen such that each branch of the capillary pair had a common arteriolar origin, venule confluence, and thus a common pressure difference across each branch, thereby eliminating the confounding effects of these variables on perfusion differences in each of the branches. Temporal and overall distributions for each parameter were determined and comparisons between paired capillaries made. Overall mean ± SEM were for D, L, V, Q, and S, respectively, 4.8 ± 0.2 μm, 161 ± 5 μm, 192 ± 5 μm/sec, 3.6 ± 0.3 pl/sec, and 43 ± 3 sec^{-1}. Symmetry between paired capillaries was assessed by parameter ratios (smaller/larger); for D, V, Q, and S, respectively, these were 0.85 ± 0.02, 0.66 ± 0.03, 0.60 ± 0.04, and 0.64 ± 0.04 with corresponding distribution medians of 0.86, 0.72, 0.63, and 0.64. Similar comparisons were made for parameters in smaller/larger diameter capillary pairs yielding for V, Q and S; 1.14 ± 0.12, 0.82 ± 0.09, and 1.37 ± 0.14 with corresponding medians of 0.9, 1.07, and 0.69. These composite results provide baseline data on the naturally occurring animal-to-animal variability, temporal variation, and overall parameter value distributions in the capillary network of this experimental model of skin microcirculation. They thus provide the necessary initial framework for subsequent assessments of pharmacological interventions and the study of various pathological processes on capillary perfusion parameters.

INTRODUCTION

The need to experimentally study *in vivo* microvascular phenomena under conditions in which the observational methods minimally affect the microvasculature has long been recognized. The skin microvasculature represents a potentially useful region for studying a variety of microcirculatory phenomena that are not necessarily related to the specialized functions of the skin circulation. In addition, recent advances in the assessment of human microvascular physiology (Ostergren and Fagrell, 1986; Tenland *et al.,* 1983; Tooke *et al.,* 1983) and pathophysiology (Fagrell *et al.,* 1984; Kimby *et al.,* 1984; Tooke *et al.,* 1985; Jacobs *et al.,* 1987) reveal the importance of understanding the interaction of capillary morphometrics

0026-2862/92 $3.00

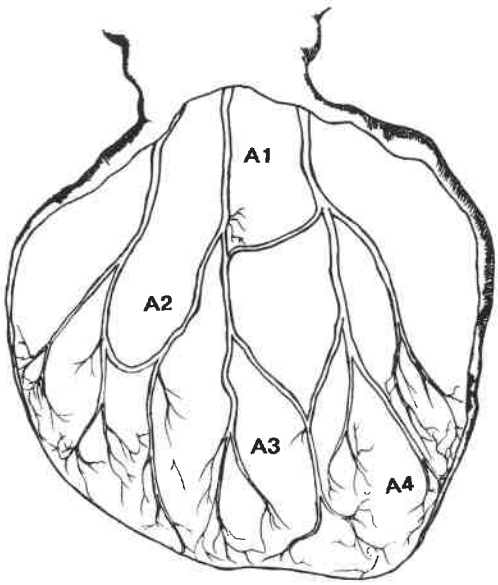

FIG. 1. Schematic rendition of the general arterial–arteriolar topography in the mouse ear. The venous–venular topography (not illustrated) is usually paired with corresponding arterial vessels. Four orders of arterial vessels branching from the entering arteries (A1 through A4) can usually be discerned. Capillary loops usually arise from the terminal arterioles.

and flow dynamics. Since some of the necessary details cannot be obtained from human studies, the use of appropriate experimental models can provide important insights. As an initial step in this process, this report is concerned with the characterization of the normal capillary geometric and blood flow features as found in the skin microvasculature of the homozygous hairless (h/h) mouse ear.

The advantages of studying the circulation using the mouse ear were first described by North and Sanders (1958), who noted that the transparency of the ear of normal white mice is sufficiently good to permit the observation of collateral circulation development following arteriolar ablation. Later the enhanced transparency present in the homozygous hairless mouse and some of its potential uses for microvascular study were described (Eriksson *et al.*, 1980) and subsequently exploited to study microcirculatory changes following scald burn injury (Boykin *et al.*, 1980). The model's uses have been extended to include the effects of frost bite injury (Bourne *et al.*, 1986), the effects of superoxide dismutase following global ischemia (Barker *et al.*, 1987), the delayed healing process of skin wounds (Bondar *et al.*, 1988), and the effects of regional ischemia and capillary flow stasis (Mayrovitz *et al.*, 1990; Sorrentino and Mayrovitz, 1991). Additional procedures and details have been recently well summarized (Barker *et al.*, 1989) and some details on the capillary network documented. The overall vascular distribution in the ear has been previously described (Eriksson *et al.*, 1980; Barker *et al.*, 1989). A sketch of the generalized distribution is shown in Fig. 1. Usually there are three arteries which provide the flow to the ear, each of which has a paired accompanying vein. At least four orders of branching can usually be discerned before the capillaries are reached. The entering arteries (labeled A1 in the figure)

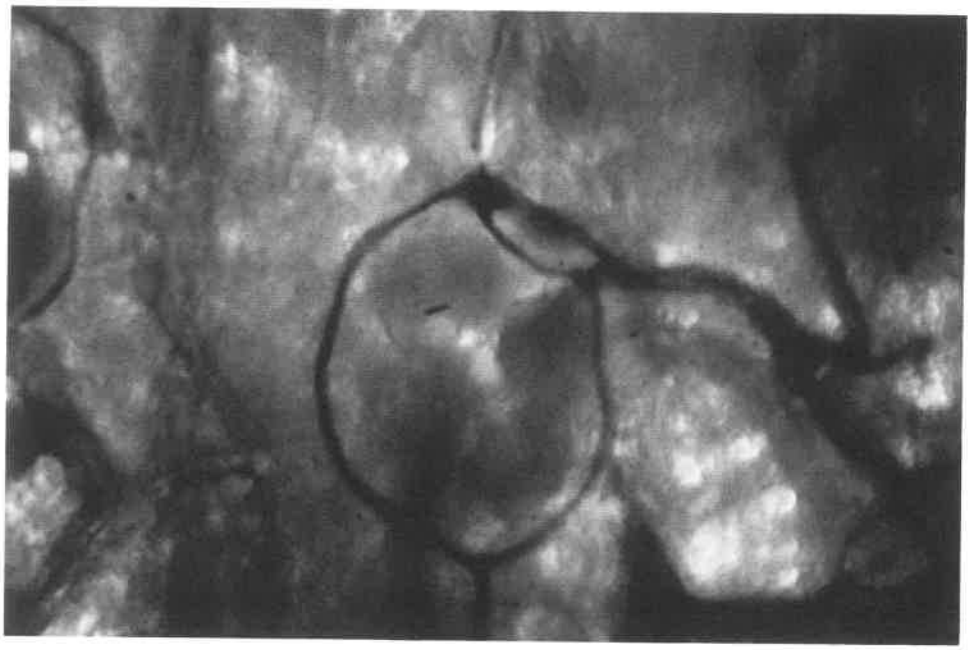

FIG. 2. Capillary loop as photographed from the TV monitor.

have been reported to have diameters of 55.5 μm (Barker *et al.,* 1989) and 35 μm (Erikkson *et al.,* 1980). The arteriolar vessels which give rise to the capillaries (A4 in the figure) have diameters reported as 13.1 and 8–9 μm by the same authors, respectively. Arteriolar arcades which connect portions of the anterior, middle, and posterior arteries have been termed "arcades" and have average diameters reported as 17.3 μm (Barker *et al.,* 1989). Systematic study of the terminal microvasculature shows that commonly, within the capillary network, two capillaries arise as a bifurcating pair at the distal end of a terminal arteriole as shown in Fig. 2. The two capillaries often circumscribe an empty hair follicle and converge to a common postcapillary junction. Similar patterns have been observed in human skin (Franzeck *et al.,* 1984). Often these capillaries give rise to offshoots which interconnect with other loops, thus forming an intricate capillary mesh. There are also pairs of bifurcating capillaries neither of which give rise to any such branches. The capillary loop thus formed constitutes what may be termed a bifurcating capillary loop. Because each of the capillaries of the loop has common arteriolar origin and venular confluence the pressure difference across each is identical. Such loops provide the opportunity for studying the details of individual capillaries as well as differences in flow dynamics in truly parallel capillaries which may differ in luminal diameter and overall length.

METHODS

Initial Procedures

Ten homozygous hairless mice (SKH-1; Charles River Laboratories), 8–10 weeks of age, weighing between 30 and 35 g were prepared for microscopic

observation of the ear microvasculature as previously described (Mayrovitz *et al.*, 1990). After anesthetic induction (pentobarbital sodium, 6 mg/100 g ip) a 25-gauge minicath (Abbott Laboratories) was inserted in the anterior intraperitoneal cavity for the administration of maintenance anesthesia. The mouse was wrapped in a 4 × 4-in. cotton gauze pad to minimize convective heat loss and placed in the supine position on an observation board. The board supported the mouse's body and had an attached standard microscope slide on which the ear was placed for microscopic observation. The ear was placed with the dorsal surface against the slide, using paraffin oil on both the dorsal and the ventral surfaces of the ear prior to placement of a No. 1 thickness microcoverslip. The coverslip weighs less than 0.1 g and was supported by the underlying oil film, thus minimizing any flow modifying effects while providing a flat surface area for microvascular study. Rectal and ear temperatures were monitored with thermistors (Bailey Instruments, Model BAT-8). Using a heat lamp, core temperature was maintained between 32 and 35° and ear temperature between 28 and 31°. Heart rate was monitored with a Photopulse Adaptor (Model PA 13) attached to the proximal portion of the tail, and data were recorded on a chart recorder.

The observation board with the mouse secured was placed on the stage of a trinocular microscope (Leitz, Laborlux) that had a calibrated zoom magnifier in the trinocular port which was coupled to a low light level TV camera (MTI Model SIT-65) and associated videocassette recorder (Panasonic Model AG-1950). Capillary loops were identified using transillumination with a 420-nm narrow band filter interposed between the light source and the condenser to enhance contrast. Figure 2 shows a typical loop as photographed from the screen of the TV monitor. The capillary loop as well as the supplying arteriole and the draining venule were visualized on the TV monitor and recorded using a 43X dry objective (NA = 0.75). Effective magnifications to the monitor were adjusted for optimum determinations of capillary length, blood velocity, and diameter and ranged from 215X for length measurements to 640X for diameter measurements. Each loop was recorded for 15 min. Using 10 mice, a total of 36 loops (72 capillaries) were studied.

Capillary Data Acquisition

The length of each capillary branch was measured from the arteriolar origin to their common venous confluence using 5 × 7-in. video prints (Mitsubishi, Model P71U). Capillary diameters were measured from the video image using a calibrated video analyzer (CVI, Model 321). Diameters and velocity were measured approximately midway between the arterial origin and the venous confluence for each capillary. At the beginning of the 15-min recording interval three diameter measurements were made, one at each cursor site (used for velocity determination) and one between the cursor locations. The average of these determinations was used for capillary diameter. Capillary blood velocity (CBV) was determined from the playback of the video recordings using the dual window video desiometric method. In this procedure, two video cursers, separated by a known distance, are inserted into the video image and positioned on the capillary, one upstream and one downstream. The video signals within these cursers, including changes in light intensity due to the flowing blood, were obtained (IPM Video Photo Analyzer 204) and the output signals transmitted to a microcomputer. Using

TABLE 1
PARAMETER VALUES AND THEIR VARIANCE ACROSS ANIMALS

Mse	n	D (μm)	V (μm/sec)	L (μm)	Q (pl/sec)	S (1/sec)
1	6	4.1 (0.9)	196 (20)	152 (54)	2.6 (0.8)	413 (171)
2	6	4.1 (1.1)	147 (43)	159 (51)	2.2 (1.5)	303 (115)
3	8	4.4 (0.5)	178 (99)	161 (40)	2.9 (1.6)	318 (164)
4	8	4.5 (0.7)	215 (82)	176 (27)	3.7 (1.9)	377 (142)
5	6	4.5 (1.1)	162 (94)	197 (25)	3.0 (2.3)	282 (147)
6	6	4.6 (1.2)	241 (118)	133 (25)	4.7 (4.6)	434 (190)
7	8	5.1 (0.9)	292 (195)	153 (44)	5.6 (3.6)	501 (391)
8	8	5.2 (0.9)	149 (70)	153 (25)	3.0 (1.3)	245 (136)
9	8	5.2 (0.9)	190 (124)	142 (24)	3.7 (2.0)	319 (240)
10	8	5.9 (1.5)	140 (49)	180 (50)	3.5 (1.5)	216 (112)
p value		0.052	0.221	0.133	0.385	0.291

Note. Mse, mouse number in order of increasing animal mean diameter D; n, number of capillaries measured; V, capillary rbc velocity; L, capillary length; Q, calculated capillary volumetric blood flow; S, calculated Newtonian wall shear rate. Data entries are animal mean values and standard deviations are in parentheses.

custom software, CBV was determined by cross-correlating the upstream and downstream signals to obtain the average transit time of the blood's optical signature. Data were automatically acquired over a sampling interval of 1 sec at a rate of 12 samples per minute, yielding 180 discrete velocity determinations in the 15-min observation interval. Individual velocity determinations with a normalized covariance less than 0.70 were rejected and the remainder was averaged to produce a single velocity value for a given capillary. The temporal variability of velocity over this time interval was assessed by calculating the coefficient of variation (CV) of the 180 velocity determinations. For each capillary, CV was calculated by computing the standard deviation (SD) of the 180 velocity values and dividing the SD by the mean of the 180 values. The CV so determined for each capillary studied in each animal was averaged to produce a single mean CV characteristic of that animal. Average volumetric blood flow was calculated as the product of measured capillary blood velocity and cross-sectional area, assuming a cylindrical shape. Newtonian wall shear rate was calculated as $8\ V/D$, where D is the mean capillary diameter. Animal-to-animal variability in measured and calculated quantities was evaluated using the mean values obtained from each animal's sampled capillaries. These data were analyzed using one-way analysis of variance procedures (ANOVA) with animal as the independent variable (factor).

RESULTS

Variability Across Animals

The means and standard deviations of capillary diameter, velocity, length, flow, and shear rate for each of the 10 animals studied are presented in Table 1. The temporal mean values obtained from each of the n capillaries of each animal were used as the primary data from which ANOVA analyses were conducted on each of the tabulated parameters. The results of the ANOVA analysis appear in the last row of the table. As shown in the table, an overall near significant difference

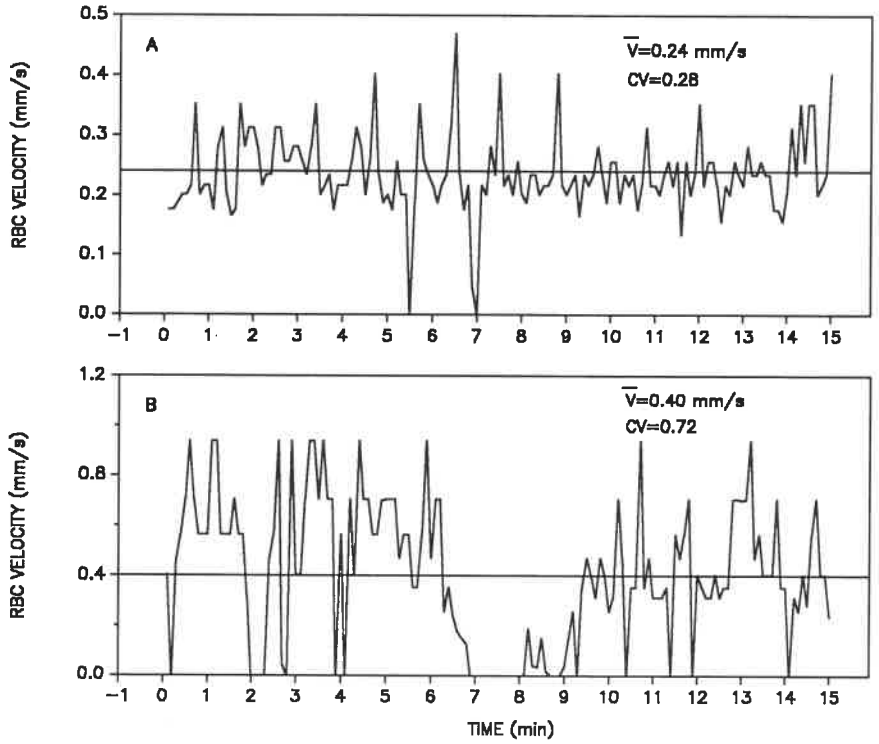

FIG. 3. Temporal variation in capillary blood velocity. Examples of time variation in CBV for two different capillaries with different time averaged means (V) and coefficients of variation (CV). Data were obtained by continuous recording of capillaries for 15 min. Solid line shows the mean value.

only in capillary diameter was found ($P = 0.052$). Neither the Scheffe nor the Tukey—HSD follow-up tests was able to detect a significant difference at the 0.05 level between any two animals. However, the Duncan multiple range test indicated a significant difference between animal 10 (which had the largest mean diameter) and the six animals with the smallest diameters (animals 1–6).

Temporal Variability in Velocity

Examples illustrating the range of temporal variability in blood velocity are shown in Fig. 3 for two different capillaries (different animals). In Fig. 3A spontaneous variations in velocity are seen to occur throughout the 15-min recording interval, which on occasion reduced capillary blood flow to zero. In Fig. 3B this variability is also present with greater variations from the mean and more numerous intervals of zero flow. The coefficients of variation (0.28 and 0.72 in this example) reflect the temporal variability which was a characteristic feature found in most capillaries measured. By tallying the duration of zero flow in all capillaries over the observation time it was found that blood velocity was reduced to zero 12.9% of the time. The animal-by-animal temporal variability as characterized by the CV and frequency of zero flow is shown in Table 2.

TABLE 2
TEMPORAL VARIABILITY IN BLOOD VELOCITY BY ANIMAL

Animal	CV	Zero flow (%)
1	0.349	5.5
2	0.258	1.1
3	0.293	1.1
4	0.758	32.1
5	0.575	16.7
6	0.471	8.9
7	0.650	21.1
8	0.797	25.6
9	0.503	11.1
10	0.463	11.1

Note. CV is the mean coefficient of variation and zero flow represents the percentage of the total observation time that zero flow was observed in each animal.

Variability in Paired Capillary Ratios

In addition to the assessment of variability in the primary parameters the variability among animals in certain of the paired ratios between smaller and larger diameter capillaries was determined. Table 3 details for each animal the ratios of diameter (D_r), velocity (V_r), flow (Q_r), shear rate (S_r), and flow fraction (FF) as determined in the smaller/larger capillary of each pair. Except for Q_r, ANOVA fails to detect any significant difference across animals. For Q_r, follow-up tests (Scheffe and Tukey) indicate the difference in Q_r is explainable by the large flow ratio in mouse 4.

TABLE 3
PAIRED CAPILLARRY PARAMETER RATIOS AND THEIR VARIANCE ACROSS ANIMALS

Mse	n	D_r	V_r	Q_r	S_r	FF
1	3	0.78 (0.05)	1.29 (1.1)	0.83 (0.7)	1.4 (1.5)	0.42 (0.18)
2	3	0.83 (0.11)	0.56 (0.1)	0.40 (0.1)	0.7 (0.1)	0.28 (0.06)
3	4	0.82 (0.15)	1.10 (0.4)	0.69 (0.1)	1.5 (0.9)	0.41 (0.02)
4	4	0.85 (0.16)	1.14 (0.4)	0.86 (0.3)	1.3 (0.5)	0.44 (0.13)
5	3	0.84 (0.10)	0.88 (0.5)	0.59 (0.3)	1.1 (0.7)	0.35 (0.14)
6	3	0.85 (0.06)	1.42 (0.4)	1.01 (0.3)	1.7 (0.5)	0.50 (0.08)
7	4	0.85 (0.16)	0.90 (0.4)	0.60 (0.2)	1.1 (0.7)	0.37 (0.10)
8	4	0.89 (0.08)	2.15 (1.1)	1.77 (1.0)	2.4 (1.2)	0.60 (0.17)
9	4	0.88 (0.08)	0.77 (0.4)	0.56 (0.2)	0.9 (0.5)	0.35 (0.10)
10	4	0.88 (0.09)	1.21 (1.1)	0.88 (0.7)	1.4 (1.5)	0.42 (0.18)
p value		0.980	0.140	0.038	0.340	0.110

Note. Ratios of diameter (D_r), velocity (V_r), flow (Q_r), shear rate (S_r), and flow fraction (FF) as determined in the smaller diameter capillary of the pair divided by the value in the larger diameter capillary. Mse, mouse number in order of increasing animal mean diameter D; n, number of capillary pairs measured. Data entries are animal mean values and standard deviations are in parentheses.

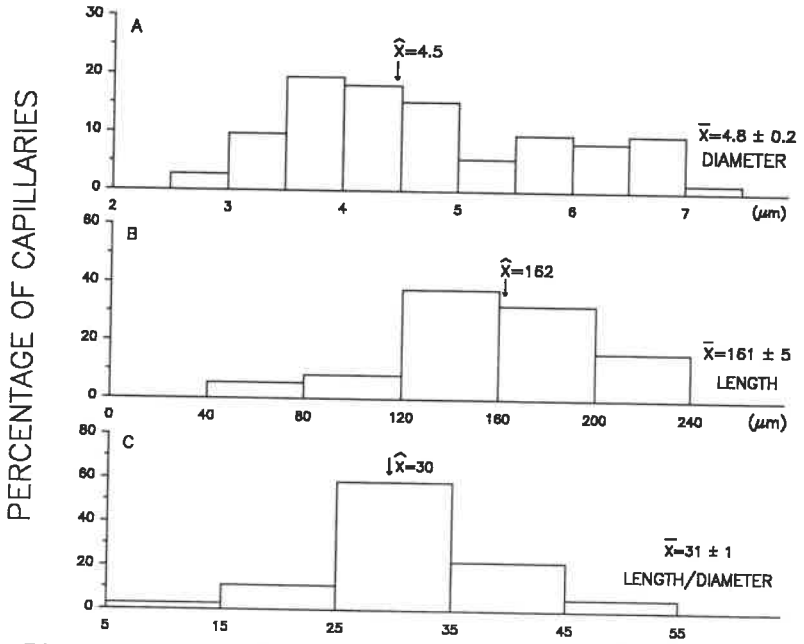

FIG. 4. Diameters and lengths of all measured capillaries (n = 72). $\hat{X}$, median and $\bar{X}$, mean ± sem.

Overall Distributions of Capillary Metrics and Hemodynamics

The diameter and length data obtained from the 72 capillaries studied are presented in Fig. 4. As may be noted in Fig. 4A, the diameter distribution is rather broad with a range of measured diameters of 2.8–7.4 μm. The median value of the distribution (4.5 μm) is less than the mean value (4.8 μm). Figure 4B shows the distribution of capillary lengths which reveals that about 75% of the capillaries lie within 120–200 μm with a median value of 162 μm. For each of the measured capillaries the ratio of its total length to its mean diameter was determined, and as shown in Fig. 4C, 60% of the capillaries had values within the range of 25 to 35 with a median value of 30 for this ratio.

Capillary blood velocity and parameters derived from it are shown in Fig. 5. In Fig. 5A the distribution of velocity as measured in the 72 capillaries is shown as a histogram. The overall range measured was quite broad ranging from 45 to 500 μm/sec. The median value (173 μm/sec) differed slightly from the mean of 192 μm/sec. In Fig. 5B the calculated volumetric blood flow is shown, and as with the velocity distribution a broad range in values (0.39–15.2 pl/sec) was found. The median value (2.8 pl/sec) differed appreciably from the mean value of 3.6 pl/sec. Figure 5C shows the distribution of wall shear rate which has a median value of 288 sec^{-1} and a mean value of 243 sec^{-1}.

Capillary Parameter Ratios

The degree of symmetry between each of the branches of the 36 capillary pairs was assessed by comparing the ratios of D_r, V_r, Q_r, and S_r. In all of these ratios the capillary parameter with the larger value is in the denominator thus making

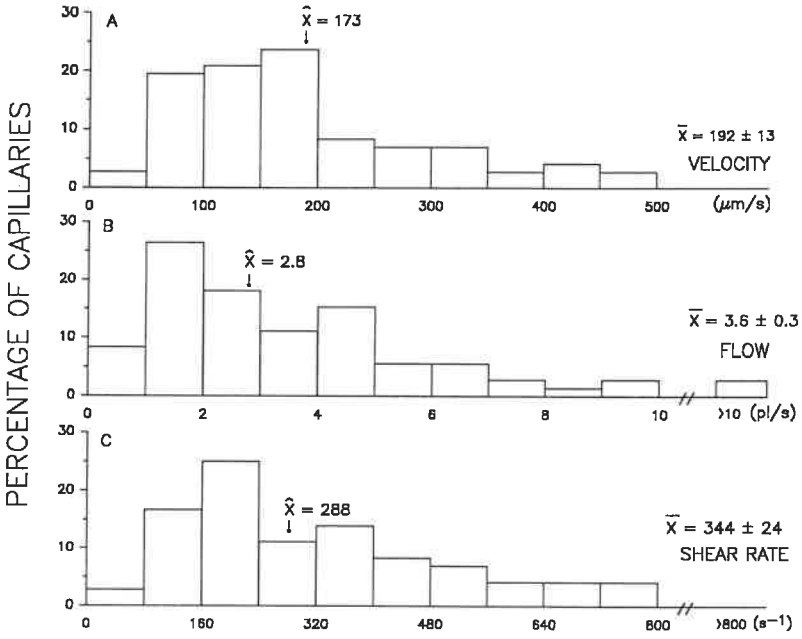

FIG. 5. Capillary blood velocity, blood flow, and shear rate.

the range of the ratio from 0 to 1. The distributions of these ratios are shown in Fig. 6. Based on the median (and mean) values of this ratio the parameter that shows the most symmetry between branches of the paired capillaries is their diameter. As may be seen in Fig. 6A, the median ratio is 0.86 with 78% of the cases being greater than 0.8. The velocity ratio is less symmetric as shown in Fig. 6B. Although the median value of 0.72 suggests moderate symmetry in this parameter, the histogram hints at a bimodal distribution with 42% of the cases having ratios less than 0.6. The medians of the distributions of Q_r and S_r as shown in Figs. 6C and 6D (0.63 and 0.64, respectively) indicate significant asymmetry in these parameters between paired capillaries. In the case of the flow distribution, the average flow entering the lower flow capillary is only 60% of its parallel pair.

To characterize the relationship between the paired capillary diameters and the various capillary flow parameters, the capillaries of each pair were categorized as smaller (D_1) and larger (D_2). In the smaller diameter capillaries ($D_1 = 4.5 \pm 0.16$ μm), flow, velocity, and shear rate were designated as Q_1, V_1, and S_1, respectively, and in the larger diameter capillaries ($D_2 = 5.2 \pm 0.2$ μm) as Q_2, V_2, and S_2. In the case of the flow distribution, the fraction of the total flow taken by the smaller capillary was designated as FF_1 and its complement, the flow fraction taken by the larger capillary, as FF_2.

Figure 7 shows the histograms obtained for the velocity and shear rate distributions. The ratios of velocity and shear rate are similar in smaller and larger diameter capillaries. Statistical evaluation using Wilcox matched-pairs signed-rank tests show no significant difference between V_1/V_2 and V_2/V_1 ($P = 0.725$) and no significant difference between S_1/S_2 and S_2/S_1 ($P = 0.232$). Similarly, there was no significant difference in the absolute values of velocity ($V_1 = 198 \pm 22$

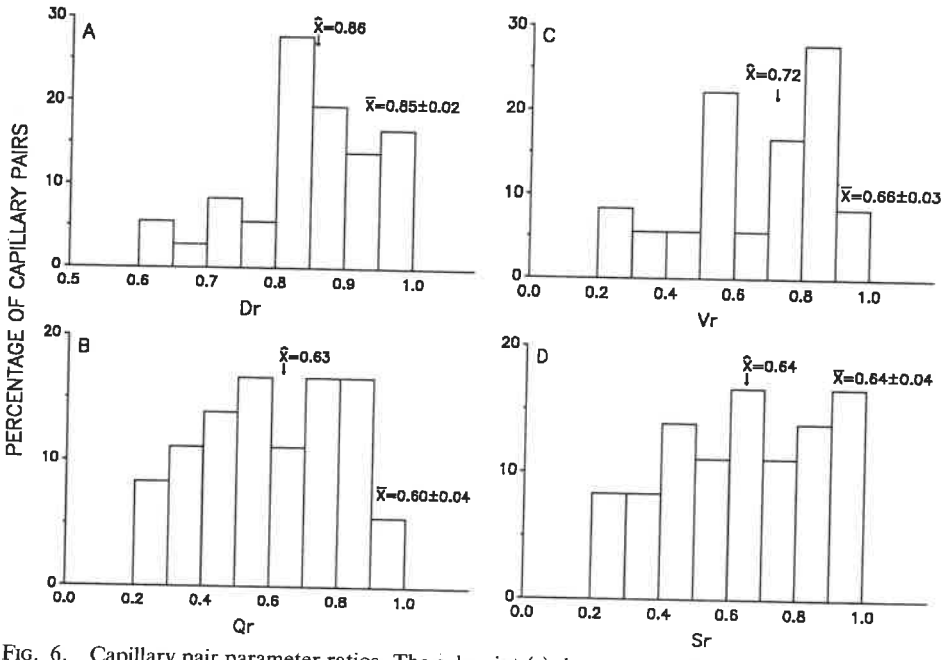

FIG. 6. Capillary pair parameter ratios. The subscript (r) denotes the ratio of the smaller to larger quantity for diameter (D_r), blood velocity (V_r), blood flow (Q_r), and shear rate (S_r) as determined in each of the bifurcating capillary pairs.

vs $V_2 = 186 \pm 15$ μm/sec, $p = 0.896$) or shear rate ($S_1 = 374 \pm 42$ vs $S_2 = 306 \pm 29$, $P = 0.215$).

Figure 8 shows the histograms obtained for the flow ratios and flow fractions. As shown in Fig. 8A, the median flow ratio in the smaller diameter capillaries was 0.69, but it is noted that in 8/36 pairs (22% of the cases) the flow ratio in the smaller diameter capillaries was greater than unity (implying a larger flow). Statistical analysis showed that the differences between Q_1/Q_2 and Q_2/Q_1 were highly significant ($P = 0.0008$) as were the differences in absolute flow ($Q_1 = 3.18 \pm 0.43$ vs $Q_2 = 4.1 \pm 0.47$ pl/sec, $P = 0.005$). As shown in Fig. 8B, the flow fraction in the smaller diameter capillary was 0.4, indicating that it received 40% of the inflow. The difference between FF_1 and FF_2 was highly significant ($P = 0.001$). Despite these differences no significant relationship between paired diameter ratios and flow ratios was demonstrable via regression analysis.

DISCUSSION

The hairless mouse has proved to be a useful and atraumatic microvascular preparation for a variety of circulatory investigations and has the potential for providing important insights into skin microcirculatory features to aid in the study and interpretation of microcirculatory derangements in skin. One of the aims of the present work was to quantitate the normally occurring distributions of the capillary metric and hemodynamic quantities. In this regard the results obtained and presented serve this purpose and thereby provide baseline information on

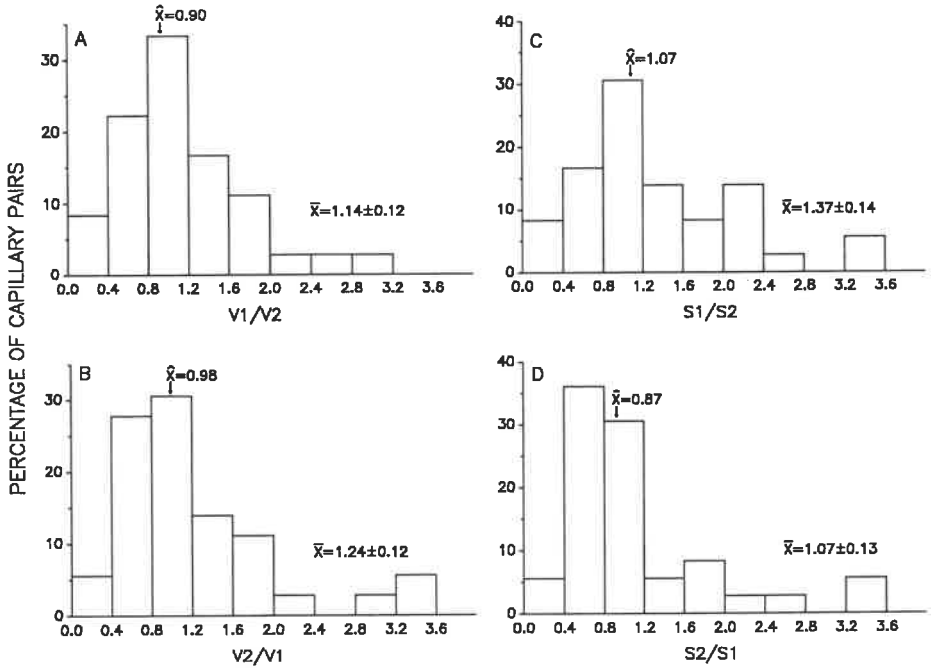

FIG. 7. Velocity (V) and shear rate (S) ratios in smaller and larger diameter capillaries of the bifurcating capillary pairs. The subscripts 1 and 2 denote the parameter value as determined, respectively, in the smaller and larger diameter capillary.

which further studies of altered physiological states and analytical modeling efforts may be firmly anchored. It is important, however, to recognize that even though the capillary network looks very similar to that seen microscopically in the perimalleolar region of human skin (Franzeck *et al.*, 1984, Fig. 3), not all features of the h/h mouse skin vasculature appear to have direct counterparts in human skin. For example papillary-like hairpin loops as typically seen in the nailfold appear not to present in the h/h mouse ear skin, although most other features including a–v shunts are present (Erikkson *et al.*, 1980). Barker and associates (Barker *et al.*, 1989) have carefully reviewed these aspects.

With regard to the baseline parameters, the present results establish that both the mean capillary diameter and the velocity in this skin microcirculation preparation are similar to those found in a variety of other tissues (Wiedeman, 1984; Zweifach and Lipowsky, 1984). Although the mean diameter herein determined (4.8 μm) is close to that reported for hamster cremaster muscle (Klitzman and Johnson, 1982), the diameters of the skin capillaries have a rather broad range from about 3 to 7.5 μm. The mean capillary blood velocity of 192 μm/sec is also similar to that found in the hamster cremaster and is also characterized by a broad range of 45 to 500 μm/sec. The value of capillary velocity herein determined is somewhat greater than the 60 μm/sec value reported by others in the same model (Barker *et al.*, 1989).

Overall capillary lengths tend to be shorter than those in the muscle microvasculature (Wiedeman, 1984). For the unbranched capillaries studied the length

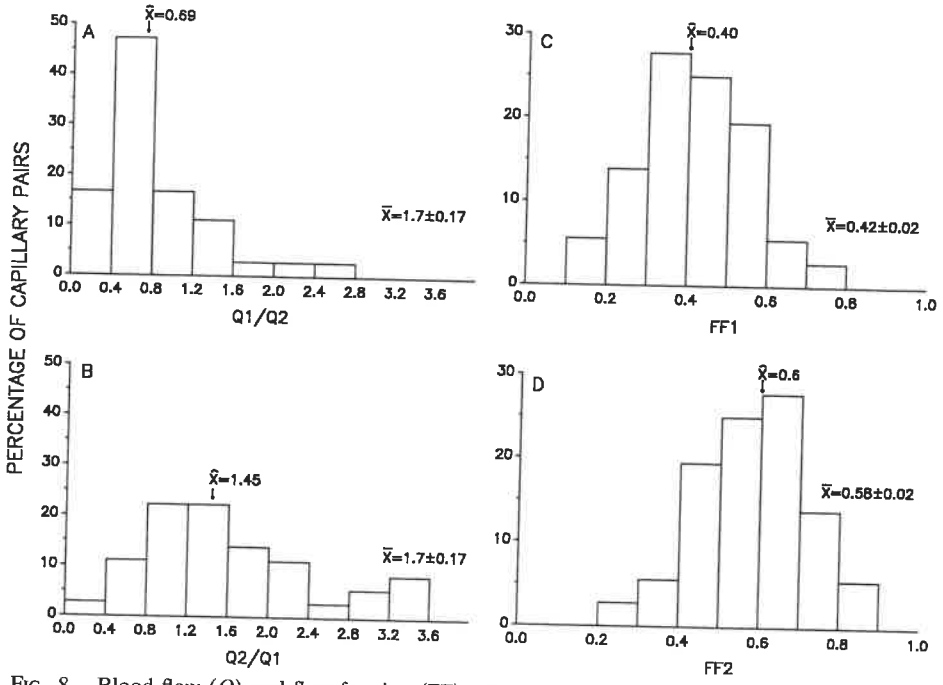

FIG. 8. Blood flow (Q) and flow fraction (FF) ratios in smaller and larger diameter capillaries of the bifurcating capillary pairs. The subscripts 1 and 2 denote the parameter value as determined, respectively, in the smaller and larger diameter capillary.

tends to be similar to the interbranch segment lengths reported in other tissues. Because of the shorter length, the ratio of capillary length to diameter in the skin capillaries tends to be smaller. Taken by itself, this finding suggests that the hydraulic hinderance of individual capillaries (L/D^4) would be less than that in longer capillaries. However, since the overall capillary network resistance to flow depends on the number and distribution of capillary–capillary anastomoses (Mayrovitz, 1986), the finding of shorter capillaries does not necessarily imply a lower capillary network resistance.

An additional important result of the present study is the systematic characterization and comparison of the geometric and flow features in adjacent paired bifurcating capillaires. Because these capillaries originate and terminate at the same arteriolar and venular sites, respectively, overall lengths of each capillary of the pair are nearly equal. Thus length as a factor in determining flow differences would be very minor. Further since the capillaries are truly in parallel, the perfusion pressure across each is equal. Thus one would anticipate that the primary determinant which would cause flow differences between these capillaries is their relative diameter. In the capillaries studied it turned out that overall, the asymmetry in diameters of paired capillaries was not large. The median value for the ratio of smaller to larger diameter (0.86) in fact seems to suggest symmetry rather than asymmetry as an average capillary property. Since the range of individual capillary diameters encountered was broad, it suggests that larger capillaries tend to be paired with the larger capillaries and smaller capillaries with smaller cap-

illaries. However in 8% of the capillary pairs studied the diameter ratio was less than 0.7, indicating that this pairing property is not uniform.

In view of the strong dependence of flow on diameter, even marginal diameter differences might be expected to give rise to significant flow asymmetry. Measurement of blood velocity showed that there was no overall significant asymmetry in this parameter. Thus the blood velocity in the arms of the capillary pairs seemed relatively insensitive to the diameter differences herein encountered. The calculated mean shear rate in the smaller diameter capillaries tended to be greater than that in the larger capillaries, although the differences were not demonstrated to be statistically significant. However, it should be noted that this calculation, which incorporates the diameter in the denominator (V/D), would tend to demonstrate elevated shear rates in the smaller diameter capillaries when, as indicated, the velocities are relatively symmetric. The volumetric blood flow partition into the bifurcating capillaries is also calculated and depends on the square of the capillary diameter. Thus, under conditions in which blood velocity in each of the paired capillaries is similar, flow to the smaller diameter branch would be expected to be less than that in the larger diameter capillary. Indeed, the data bear this out as an average finding, with the flow in the smaller diameter capillary being significantly less than that in the paired, larger capillary. However, in about 20% of the capillary pairs studied, the blood flow in the smaller diameter capillary was greater. Since these capillaries had the same length, factors other than capillary diameter must predominate in these cases in determining the capillary blood flow partitioning.

The present results also provide new information on the naturally occurring variability in capillary blood velocity. As exemplified in Fig. 3, CBV is characterized by significant variations about its mean value with either transient or more extended intervals of zero flow. All animals showed some intervals of zero flow with a large quantitative difference among animals ranging from 1.1 to 25.6% of the total observation time. The overall mean indicates that these skin capillaries have zero flow 12.9% of the time. Such zero flow states may be attributable to transient blockage by circulating white blood cells as has been noted in other microvascular beds (Bagge *et al.*, 1980; Engler *et al.*, 1983; Mayrovitz *et al.*, 1987). The calculated coefficients of variation which ranged from 0.26 to 0.80 reflect this variation in percentage of zero flow as well as other sources of temporal variation. Despite significant temporal variation in some animals, the overall mean velocity (and parameters derived from it) did not significantly differ among animals. Although these findings do not explain the source of velocity variation they serve to establish the range of applicability of the present model when capillary blood velocity is a primary quantity of interest. Such would be the case when the model is used to assess the effects of pharmacological interventions or pathological processes on capillary perfusion parameters.

ACKNOWLEDGMENTS

The technical assistance provided by Ronald Sampsell, DVM, is gratefully acknowledged. This research was supported in part by the Juvenile Diabetes Foundation International, Grant 1891090.

REFERENCES

BAGGE, U., AMUNDSON, B., AND LAURITZEN, C. (1980). White blood cell deformability and plugging of skeletal muscle capillaries in hemorrhagic shock. *Acta Physiol. Scand.* **108,** 159–163.

BARKER, J., BARTLETT, R., FUNK, W., HAMMERSEN, F., AND MESSMER, K. (1987). The effect of superoxide dismutase on the skin microcirculation after ischemia and reperfusion. *Prog. Appl. Microcirc.* **12,** 276–2781.

BARKER, J. H., HAMMERSON, F., BONDER, I., AND MESSMER, K. (1989). The hairless mouse ear for in vivo studies of skin microcirculation. *Plast. Reconst. Surg.* **83,** 948–959.

BONDAR, I., BARKER, J. H., GALLA, TH., UHL, E., AND MESSMER, K. A. (1988). A new model to study microcirculatory changes during wound healing in the skin. *Int. J. Microcirc.* **7,** 175–181.

BOURNE, M. H., PIEPKORN, M. W., CLAYTON, F., AND LEONARD, L. G. (1986). Analysis of microvascular changes in frostbite injury. *J. Surg. Res.* **40,** 26–35.

BOYKIN, J. V., ERIKSSON, E., AND PITTMAN, R. N. (1980). In vivo microcirculation of a scald burn and the progression of post burn dermal ischemia. *Plast. Reconstr. Surg.* **66,** 191–198.

ENGLER, R. L., SCHMID-SCHOENBEIN, G. W., AND PAVELEC, R. S. (1983). Leukocyte capillary plugging in myocardial ischemia and reperfusion in the dog. *Am. J. Pathol.* **111,** 98–111.

ERIKSSON, E., BOYKIN, J., AND PITTMAN, R. N. (1980). Method for *in vivo* microscopy of the cutaneous microcirculation of the hairless mouse ear. *Microvasc. Res.* **19,** 374–379.

FAGRELL, B., HERMANSSON, I. L., KARLANDER, S. G., AND OSTERGREN, J. (1984). Vital capillary microscopy for assessment of skin viability and microangiopathy in patients with diabetes mellitus. *Acta Med. Scand. (Suppl).* **687,** 25–28.

FRANZECK, U. K., BOLLINGER, A., RENATE, H., AND HUCH, A. (1984). Transcutaneous oxygen tension and capillary morphologic characteristics and density in patients with chronic venous incompetence. *Circulation* **70,** 806–811.

JACOBS, M. J., SLAAF, D. W., LEMMENTS, A. J., AND RENEMAN, R. S. (1987). The use of hemorheological and microcirculatory parameters in evaluating the effect of treatment in Raynaud's phenomenon. *Vasc. Surg.* **21,** 9–15.

KIMBY, E., FAGRELL, B., BJORKHOLM, M., HOLM, G., MELLSTEDT, AND NORBERG, R. (1984). Skin capillary abnormalities in patients with Raynaud's phenomenon. *Acta Med. Scand.* **215,** 127–134.

KLITZMAN, B., AND JOHNSON, P. C. (1982). Capillary network geometry and red cell distribution in hamster cremaster muscle. *Am. J. Physiol.* **242,** H211–H219.

MAYROVITZ, H. N. (1986). Hemodynamic significance of microvascular arteriolar anastomosing. *In* "Microvascular Networks: Experimental and Theoretical Studies" (A. S. Popel, and P. C. Johnson, Eds.), pp. 197–209. Karger, Basel.

MAYROVITZ, H. N., KANG, S. J., HERSCOVICI, B., AND SAMPSELL, R. N. (1987). Leukocyte adherence initiation in skeletal muscle capillaries and venules. *Microvasc. Res.* **33,** 22–34.

MAYROVITZ, H. N., MOORE, J., AND SORRENTINO, E. A. (1990). A model of regional microvascular ischemia in intact skin. *Microvasc. Res.* **39,** 390–394.

NORTH, K. A. K., AND SANDERS, A. G. (1958). The development of collateral circulation in the mouse ear. *Circ. Res.* **6,** 721–727.

OSTERGREN, J., AND FAGRELL, B. (1986). Skin capillary blood cell velocity in man: Characteristics and reproducibility of the reactive hyperemia response. *Int. J. Microcirc. Clin. Exp.* **5,** 37–51.

SORRENTINO, E. A., AND MAYROVITZ, H. N. (1991). Skin capillary reperfusion after regional ischemia. *Int. J. Microcirc. Clin. Exp.* **10,** 105–115.

TENLAND, T., SALERUD, E., NILSSON, G. E., AND OBERG, F. A. (1983). Spatial and temporal variations in human skin blood flow. *Int. J. Microcirc. Clin. Exp.* **2,** 81–90.

TOOKE, J. E., LINS, P. E., OSTERGREN, J., AND FAGRELL, B. (1985). Skin microvascular autoregulatory responses in type I diabetes: The influence of duration and control. *Int. J. Microcirc. Clin. Exp.* **4,** 249–256.

TOOKE, J. E., OSTERGREN, J., AND FAGRELL, B., (1983). Synchronous assessment of human skin microcirculation by laser Doppler flowmetry and dynamic capillaroscopy. *Int. J. Microcirc. Clin. Exp.* **2,** 277–284.

WIEDEMAN, M. P. (1984). Microvascular architecture. *In* "Handbook of Physiology, The Cardiovascular System. (E. M. Renkin and C. C. Michel, Eds.), Vol. 4, Part 1, pp. 11–40. American Physiology Society, Bethesda, MD.

ZWEIFACH, B. F., AND LIPOWSKY, H. H. (1984). Pressure–flow relationships in blood and lymph microcirculation. *In* "Handbook of Physiology, The Cardiovascular System. (E. M. Renkin and C. C. Michel, Eds.), Vol. 4, Part 1, pp. 251–307. American Physiology Society, Bethesda, MD.